Analytical Investigation of Water Transport

Sukkee Um† · Kwan-Soo Lee* · Hye-Mi Jung**

Key Words : Analytical Investigation, Water Transport, Polymer Electrolyte Fuel Cells

Abstract

Comprehensive analytical models focusing on the anode water loss, the cathode flooding, water equilibrium, and water management strategy are developed for polymer electrolyte fuel cells. Analytical solutions presented in this study are compared with two-dimensional computational results and shows a good agreement in predicting those critical characteristics of water. General features of water concentration profile as a function of membrane thickness and current density are presented to illustrate the net effect of the back-diffusion of water from the cathode to anode and the water production by the cathode catalytic reaction on water transport over a fuel cell domain. As one of practical applications, the required humidity level of feed streams for full saturation at the channel outlets are investigated as a function of the physical operating condition. These analytical models can provide good understanding on the characteristic water

Nomenclature

A	Area, cm^2
$A_{x,c}$	gas channel cross-sectional area, cm^2
a	water activity
c	molar concentration, mol/cm^3
D	mass diffusivity of species, cm^2/sec
EW	equivalent weight of membrane
F	Faraday constant, C/e-mol
I	current density, A/cm^2
J	back-diffusion of water
j	transfer current, A/cm^3
L	gas channel length, cm
n	molar flow rate, $mol/cm^3 \cdot sec$
n_a	2, number of electrons per H2 molecule
n_c	4, number of electrons per O2 molecule
n_d	electro-osmotic drag coefficient
P	pressure, Pa
Q	volumetric flow rate, cm^3/sec
R	gas constant, 8.314 J/mol·K
RH	relative humidity
t	membrane thickness
T	temperature, K
v	velocity, cm/sec
X	mole fraction
y	axial location

1. Introduction

It is widely recognized that an in-depth study of the water balance across the membrane electrode assembly (MEA) of polymer electrolyte fuel cells is of extremely importance to achieve the optimal performance in a fuel cell engine. For instance, the full humidification of reactant gas streams might cause the cathode flooding by the cathode catalytic reaction which interrupts the mass transport process of oxidant flow through the gas diffusion layer (GDL), resulting in the mass transport limitation on a cell polarization curve. While for gas streams with low humidity at the gas channel inlets, the anode/membrane interface loses the water molecules by the electro-osmotic drag, causing the ionomer membrane more resistive to the protonic flow. Therefore, water balance is one of the significant considerations in the design of polymer electrolyte fuel cells.

Remarkable mathematical models for water balance in proton exchange membrane (PEM) fuel cells have been proposed to identify the water transport phenomena and facilitate the experimental study in the open literature.[1-3] These models are one-dimensional and the membrane remains fully saturated or low humidified for effective water management study. The use of the detailed experimental data of diffusion and electro-osmotic drag coefficients of water in Nafion® 117 membranes has been made by Springer et al.[4,5] in order to predict the steady-state water profile and resulting ionic conductivity. Multi-dimensional fuel cell modeling in two- or three-dimension were also made coupling the water transport with other transport phenomena and the electrochemical-kinetics [1-3, 6-11] in efforts to present more extensive water management model which, however, requires large scale computing capability and rather time consuming processes. Aside these extensive numerical models, theoretical pre-estimation focusing on water transport in PEM fuel cells can be greatly utilized to grasp dominant water transport mechanism under a given

† Member, Hanyang University
E-mail : sukkeeum@hanyang.ac.kr
TEL/FAX : (02)2220-0432
* Hanyang University
** Graduate School of Hanyang University

operating condition in a simplified manner. It can also be used to determine optimal system parameters ensuring well-balanced water distribution over a fuel cell domain with hands-on calculation.

Based on the aforementioned purpose, the present work is intended to present an analytical study of water transport, which examines various water transport regimes of practical interest, such as anode water loss and cathode flooding, and proposes a continuous stirred fuel cell reactor (CSFCR) model for limiting situations where anode and cathode water profiles acquire an equilibrium state. The anode water loss location at the anode/membrane interface along the gas channel is computed as a function of the various operating parameters at which a fuel cell shows the highest ionic resistance in the Nafion® membrane. The cathode flooding point at the cathode/membrane interface is also predicted along with the anode water loss location. The water activity at the gas channel outlet is also obtained by employing the continuous stirred tank fuel cell model which is applicable to the advanced thinner electrolyte membrane. With the CSFCR model, it can be determined whether the amount of the water along the outlet boundary of a fuel cell system reaches the saturation level or not. Moreover, a particular water management strategy is introduced to suggest appropriate humidity levels of the inlet feed streams, reaching fully saturated state at the channel outlets as a function of various operating parameters: pressure, temperature, and so on.

2. Analytical Study of Water Transport

2.1 Characteristics of Water Concentration

Typical water concentration profiles in the anode and cathode along the flow direction are depicted in Fig. 1. Interesting characteristics include zero water flux across the membrane and hence the minimal point in the anode water profile, the onset of cathode flooding where water vapor becomes saturated, and the equilibrium of the water activity between the anode and

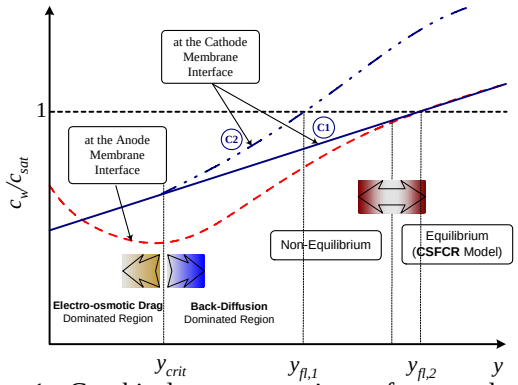

Fig. 1 Graphical representation of general water concentration profiles along the flow direction in both anode and cathode, showing various regimes of water transport and the region of applicability of the CSFCR model

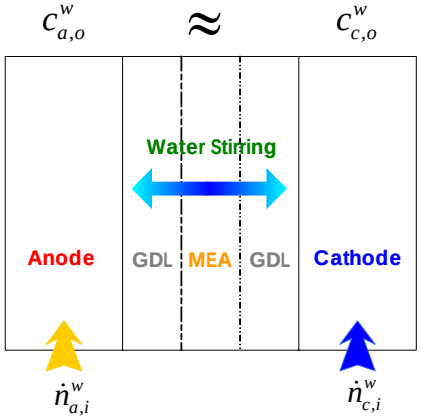

Fig. 2 Schematic diagram of a continuous stirred fuel cell reactor for water transport analysis

cathode at the outlets where the continuous stirred fuel cell reactor (CSFCR) model is applicable as illustrated in Fig. 2. As shown in Fig. 1, the water concentration at the anode/membrane interface decreases along the axial direction and then reaches the minimal point at which the net water flux across the membrane becomes zero, implying that the electro-osmotic drag is balanced by the back-diffusion of water. The location, y_{crit}, in Fig. 1 indicates this zero net water flux location. Before this critical location, the anode is characterized by water loss and after it the anode gains water. The anode can be fully dehydrated if the back-diffusion from the cathode is not strong enough to compensate the anode water loss by the electro-osmotic drag in the worst scenario. This critical location is also important in that it signifies the most resistive location of the membrane.

For current densities high enough for abundant water production, water is produced in the cathode such that the gas is saturated with water vapor and vapor-to-liquid phase change is imminent, which brings about cathode flooding. Theoretically, liquid water appears at a flooding point, y_{fl}, shown in Fig. 1.

When a thin membrane is used in fuel cells, the water exchange between the anode and cathode is greatly facilitated, thereby resulting in the water concentration on the anode and cathode sides of the membrane approaching each other towards the exit, a state called “equilibrium.” This is depicted as the curve C1 in Fig. 1. This equilibrium condition occurs only when the back diffusion of water through the membrane is largely dominating. However, if the membrane is sufficiently thick that back-diffusion of water cannot compensate for the electro-osmotic drag of water, the differential in the water concentration between the anode and cathode gets widened as a result of water production on the cathode side. This is shown as the curve C2 in Fig. 1.

2.2 Water Loss

This section presents an analytical solution for the critical anode location where zero net water flux or equivalently the minimum anode water concentration occurs. This analysis is of great importance for water

control in PEM fuel cells, as it determines whether or not the anode feed stream can gain water from the cathode at given operating conditions.

A conservative estimate of the zero net flux location and the extent of anode water loss is to assume that the water diffusion through the membrane is negligible as compared to water drag before reaching the zero net flux point. Such an analytical estimated is performed below. The water and total gas molar flow rates in the anode can be calculated, respectively, by

$$\dot{n}_a^W = \dot{n}_{a,i}^W - \dot{n}_{a,d}^W \quad (1)$$

$$\dot{n}_a^{total} = \dot{n}_{a,i}^{total} - \dot{n}_{a,d}^W - \dot{n}_{a,cons}^{H2} \quad (2)$$

Similarly, the water and the total gas molar flow rates at the zero net water flux location in the cathode can be calculated as

$$\dot{n}_c^W = \dot{n}_{c,i}^W + \dot{n}_{c,d}^W + \dot{n}_{c,p}^W \quad (3)$$

$$\dot{n}_c^{total} = \dot{n}_{c,i}^{total} + \dot{n}_{c,d}^W + \dot{n}_{c,p}^W - \dot{n}_{c,cons}^{O2} \quad (4)$$

If the electro-osmotic drag and the back-diffusion of water are assumed to balance each other beyond the zero net flux point, an analytical estimate of where cathode flood occurs can be made.

When the water concentration in vapor phase reaches the saturation value which means the flooding in the cathode gas channel, i.e. $c_c^W = c^{W,sat}$ at $y = y_{fl}$, the critical flooding location, y_{fl} in the cathode channel along the axial direction can be calculated,

$$c^{W,sat} v_{c,bulk} A_{x,c} = \dot{n}_{c,i}^W + n_d \frac{I_{cell}}{F} A_{rx,crit} + \frac{I_{cell}}{2F} A_{rx,fl} \quad (5)$$

When a thin electrolyte membrane is used for a fuel cell, water exchange between anode and cathode is greatly enhanced due to fast diffusion through the thin membrane, rendering the water activity values to be equal between the two sides of the membrane, a state of equilibrium for water balance between anode and cathode. Under this equilibrium state as depicted in Fig. 2, the water activity values at the anode and cathode outlets are the same, making the fuel cell essentially a "Continuous Stirred Fuel Cell Reactor (CSFCR)". It consists of two flow channels for the anode and cathode feed streams and a thin membrane electrode assembly (MEA) in between. In a typical Continuous Stirred Tank Reactor (CSTR) model, all reactants entering a chemical reactor well mix and react to form products of uniform concentration at the exit. The CSTR concept is extended below to fuel cells for an analytical estimate of water activity towards the anode and cathode exits.

The total molar flow rate entering the anode gas chamber can be computed by the stoichiometry definition; i.e.

$$\dot{n}_{a,i}^{total} = \frac{\zeta_a \cdot I_{ref} \cdot A_{rx}}{2F\left[\left(1 - X_{a,i}^{N2}\right) - \frac{P^{sat}}{P_{a,i}} \cdot RH_{a,i}\right]} \quad (6)$$

where $\dot{n}_{a,i}^{total}$ is the total molar flow rate at the anode gas channel inlet.

Similarly, the total molar flow rate for the cathode feed stream is given by,

$$\dot{n}_{c,i}^{total} = \frac{\zeta_c \cdot I_{ref} \cdot A_{rx}}{4F\left[\left(1 - X_{c,i}^{N2}\right) - \frac{P^{sat}}{P_{c,i}} \cdot RH_{c,i}\right]} \quad (7)$$

where $\dot{n}_{total,i}^{c}$ is the total molar flow rate at the cathode gas channel inlet.

The overall electrochemical reaction for a fuel cell system is found,

$$2H_2 \quad + \quad O_2 \quad \square \quad 2H_2O \quad (8)$$

$$\left(\zeta_a \frac{I_{ref}}{2F} - \frac{I_{cell}}{2F}\right)\left(\zeta_c \frac{I_{ref}}{4F} - \frac{I_{cell}}{4F}\right)\left(\dot{n}_{a,i}^W + \dot{n}_{c,i}^W + \frac{I_{cell}}{2F}\right) \quad (9)$$

Equation (9) describes the net molar flow rate change by the overall fuel cell reaction.

The total molar flow rate of water supplied to the anode and the cathode feed streams and produced by the oxygen reduction reaction should be equal to the partial water molar flow rate out of the total molar flow rate considering the over-all molar flow rate change as in Eq. (9),

$$\left(\dot{n}_{a,o}^{total} + \dot{n}_{c,o}^{total}\right) \cdot X_o^W = \dot{n}_{a,i}^W + \dot{n}_{c,i}^W + \dot{n}_{c,p}^W \quad (10)$$

3. Results and Discussion

A set of theoretical calculations are made using the analytical solutions developed in this work and these analytical results are compared to the two-dimensional computer simulations for qualitative validation. First, additional two-dimensional simulation plots using the computational fuel cell dynamics (CFCD) program are presented to develop a basic understanding of water transport. Theoretical predictions are introduced in detail thereafter.

Fig. 3 displays the numerically predicted water concentration profiles in the through-membrane direction at two different current densities. Fully humidified fuel and dry air enter the gas channels in a co-flow manner. At the low operating current density ($I_{cell} = 0.23$ A/cm^2) as shown in Fig. 3(a), the water concentration on the anode/membrane interface is seen to be higher than that on the cathode near the channel inlet, i.e. up to $y = L/4$. This is indicative of forward water diffusion from anode to cathode through the membrane. However, the water concentration in the in-plane direction then gradually decreases by this forward-diffusion and the electro-osmotic water loss, while there is water buildup at the cathode/membrane interface due mainly to the oxygen reduction reaction (ORR). In the middle section of the fuel cell (i.e. $y = L/2$), the diffusion of water through the membrane switches the direction, transporting water from the cathode back to anode. Fig. 3(b), however, illustrates a remarkably different feature of water transport when the current density is close to the typical maximum power density ($I_{cell} = 1.17$ A/cm^2). First, there is a significant concentration gradient across the membrane because the mass diffusivity of water in the

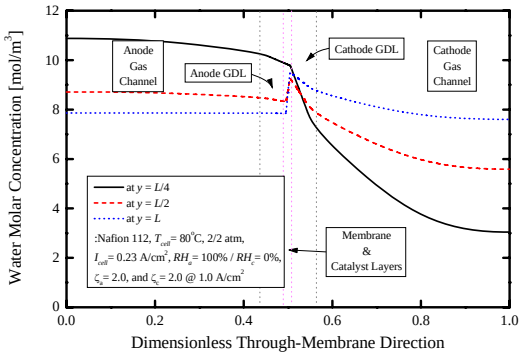

(a) water molar concentration @ $I_{cell} = 0.23$ A/cm^2

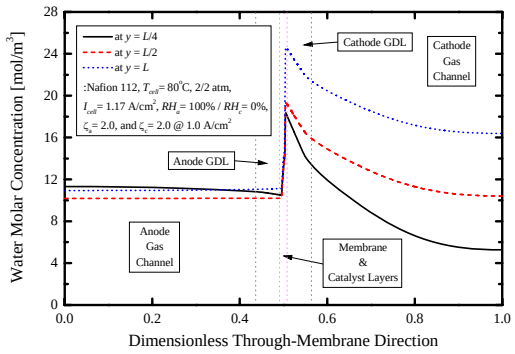

(b) water molar concentration @ $I_{cell} = 1.17$ A/cm^2

Fig. 3 Computed water concentration profiles in PEM fuel cells: (a) $I_{cell} = 0.23$ A/cm^2, and (b) $I_{cell} = 1.17$ A/cm^2

membrane is two orders of magnitude smaller than that in other regions. Water diffusivity in the electrolyte phase is an adversely self-recursive function of water concentration. Therefore, most of water produced by the catalytic reaction escapes through the cathode GDL and the neighboring gas channel. Secondly, strong back-diffusion of water due to high water buildup at the cathode/membrane interface minimizes the anode water

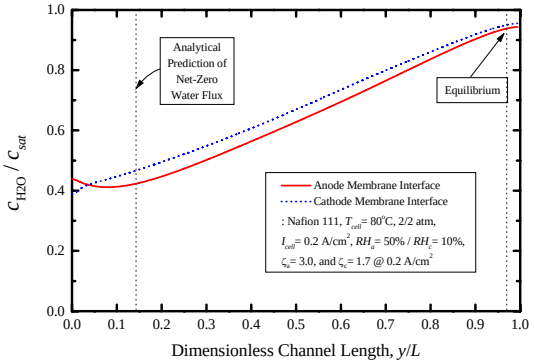

Fig. 4 Two-dimensional results of the dimensionless water concentration profiles along the flow direction and comparison with the theoretical prediction of the anode zero net flux location in a Nafion® 111 fuel cell

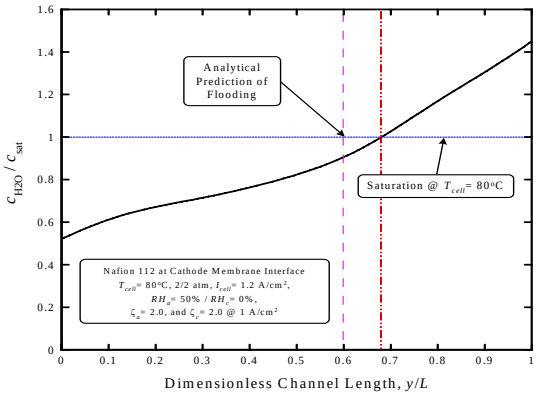

Fig. 5 Two-dimensional simulation result of the dimensionless water concentration profile on the cathode side and the theoretical prediction of cathode flooding location in a Nafion® 112 fuel cell

loss and therefore the variation of water concentration in the anode channel is negligibly small. At the anode channel exit, the water concentration is even slightly greater than that at $y = L/2$ with the help of back-driven water diffusion.

Fig. 4 displays the axial profiles of dimensionless water concentration at the anode/membrane and cathode/membrane interfaces as predicted from two-dimensional simulations, along with an analytical prediction of the minimum anode water content location for a low humidification case (RH_a = 50% and RH_c = 10%) with a thin membrane of Nafion® 111. It is shown Fig. 4 that the theoretical estimate of the anode net-zero water flux location is in good agreement with the two-dimensional simulation. Moreover, the water molar concentrations at the anode/ and cathode/membrane interfaces approach each other towards the exit of the gas channel, demonstrating the equilibrium state of water across thin membranes as schematically shown in Fig. 2.

Fig. 5 compares an analytical prediction of the cathode flooding location with the two-dimensional simulation at high current density ($I_{cell} = 1.2$ A/cm^2) at which water concentration on the cathode exceeds saturation level. Because the back-diffusion of water was neglected in the flooding location analysis, it was necessary to rather choose a thick membrane for comparison than the thin membrane as used for Fig. 4. The analytical solution predicts a slightly earlier cathode flooding location in the cathode than that estimated by the two-dimensional numerical simulation ($y_{fl,theo} \approx 0.6$ and $y_{fl,simul} \approx 0.68$, respectively).

Fig. 6 compares the predicted water molar concentrations at the exits of gas channels by the two-dimensional computational results and the analytical solution, respectively at low current density, $I_{cell} = 0.2$ A/cm^2. A thin (Nafion® 111) and a thick (Nafion® 115)

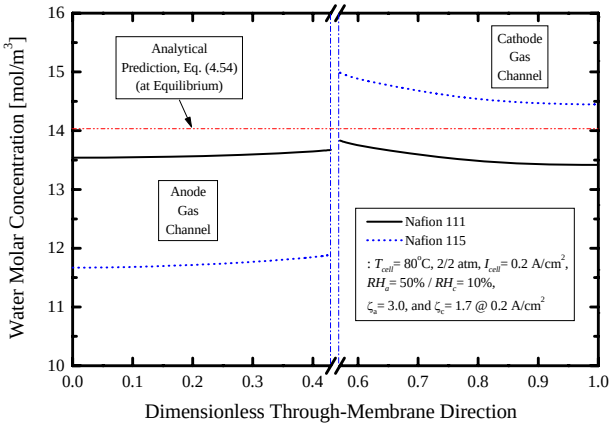

Fig. 6 Two-dimensional simulation results of the water concentration profiles at both anode and cathode outlets in Nafion® 111 and Nafion® 115 fuel cells and comparison with the theoretical prediction of the water concentration at the channel outlets using CSFCR model

membranes are used in order to elucidate the validity range of CSFCR model that hinges upon the equilibrium condition of water between the anode and cathode outlets.

As expected, the thin membrane case maintains nearly the same water concentration at both anode and cathode outlets and the analytical estimation using CSFCR model is close to the two-dimensional computational water molar concentration profiles. On the contrary, for the thick membrane, there exists a large difference in the water molar concentration between the anode and cathode outlets. This becomes obvious in Fig. 7 which displays axial profiles of the dimensionless water molar concentration in the flow direction. The difference in the water concentration between the anode and cathode grows larger for the thick membrane along the feed stream due to reaction water buildup on the cathode side, while the thin membrane shows an equilibrium state towards the end of the channel length.

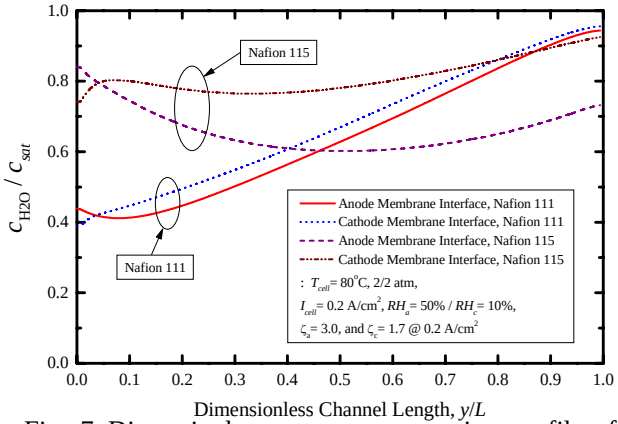

Fig. 7 Dimensionless water concentration profiles for equilibrium and non-equilibrium states of water in PEM fuel cells

4. Conclusion

In summary, the theoretical solutions are successfully and provide good estimation of the critical locations for anode water loss and cathode flooding under the various operating conditions in PEM fuel cells. The analytical solutions are compared to the previously developed two-dimensional computational results for in-depth discussion on the critical water transport characteristics. The CSFCR model developed in this study shows unique feature of water equilibrium accounting for the effects of the membrane thickness and operating current density on the water concentration at both anode and cathode outlets. The CSFCR model can be used to calculate the water activity at the channel outlets when the thin membranes (i.e. ~ 20 μm) are used.

References

(1) A. Rowe, X. Li, 2001, "Mathematical Modeling of Proton Exchange Membrane Fuel Cells," *J. Power Sources*, vol. 102, pp. 82-96

(2) T. Okada, G. Xie, and M. Meeg, 1998, "Simulation for water management in membranes for polymer electrolyte fuel cells," *Electrochimica Acta*, vol. 43, pp. 2141-2155

(3) N. Djilali, and D. M. Lu, 2002, "Influence of heat transfer on gas and water transport in fuel cells," *Int. J. of Thermal Sciences*, vol. 41, pp. 29-40

(4)] T. E. Springer, T. A. Zawodinski, and S. Gottesfeld, 1991, "Polymer Electrolyte Fuel Cell Model," *J. Electrochem. Soc.*, vol. 136, pp. 2334-2342

(5) T. E. Springer, M. S. Wilson, S. Gottesfeld, 1993, "Modeling and Experimental Diagnostics in Polymer Electrolyte Fuel Cells," *J. Electrochem. Soc.*, vol. 140, pp. 3513-3526

(6) D. M. Bernardi, 1990, "Water Balance Calculation for Solid-Polymer-Electrolyte Fuel Cells," *J. Electrochem. Soc.*, vol. 137, pp. 3344-3350

(7) H. Voss, D. Wilkinson, D., P. Pickup, M. Johnson, and V. Basura, 1995, "Anode water removal: a water management and diagnostic technique for solid polymer fuel cells," *Electrochimica Acta*, vol. 40, pp. 321-328

(8) T. F. Fuller, J. Newman, 1993, "Water and Thermal Management in Solid-Polymer Electrolyte Fuel Cells," *J. Electrochem. Soc.*, vol. 140, pp. 1218-1225

(9) T. V. Nguyen, R. E. White, 1993, "A Water and Heat Management Model for Proton Exchange Membrane Fuel Cells," *J. Electrochem. Soc.*, vol. 140, pp. 2178-2186

(10) J. S. Yi, T. V. Nguyen, 1999, "Multicomponent Transport in Porous Electrodes of Proton Exchange Membrane Fuel Cells Using the Interdigitated Gas Distributors," *J. Electrochem. Soc.*, vol. 146, pp. 38-45

(11) I I.-M. Hsing, and P. Futerko, 2000, "Two-dimensional simulation of water transport in polymer electrolyte fuel cells," *Chemical Engineering Science*, vol. 55, pp. 4209-4218